Cumulative impact assessment of tidal stream energy extraction in the Irish Sea

David Haverson[a,*], John Bacon[a], Helen C.M. Smith[b], Vengatesan Venugopal[c], Qing Xiao[d]

[a] Centre for Environment, Fisheries and Aquaculture Science, Lowestoft NR33 0HT, United Kingdom
[b] College of Engineering, Mathematics and Physical Sciences, University of Exeter, Falmouth TR10 9EZ, United Kingdom
[c] Institute of Energy Systems, University of Edinburgh, Edinburgh EH9 3DW, United Kingdom
[d] Department of Naval Architecture, University of Strathclyde, Glasgow G1 1XQ, United Kingdom

ARTICLE INFO

ABSTRACT

A cumulative impact assessment of tidal stream developments in the Irish Sea has been conducted on a high-resolution depth-averaged hydrodynamic model, using Telemac2D. Eight sites were investigated, representing the proposed developments at the time of study. These included: Ramsey Sound, Anglesey, Strangford Loch, Mull of Kintyre, Torr Head, Fair Head, Sound of Islay and West of Islay. Only three projects showed array-array interaction: Fair Head, Torr Head and Mull of Kintyre. A smaller model domain was created for further analysis. Results showed Mull of Kintyre had little impact. Fair Head reduced the energy production at Torr Head by 17%, whereas, Fair Head only reduced by 2%. This was caused by the tidal asymmetry whereby the flood was stronger. When operated concurrently, the maximum power-output at Torr Head is 64.5 MW, representing 31% reduction. If Torr Head can still operate commercially in the presence of Fair Head, then the additional environmental impact of Torr Head, such as the change in bed shear stress, is small. Within the Irish Sea, very few of the tidal projects investigated are geographically close to each other. As the industry develops, the risk of interaction to these sites will grow when more intermediary sites are developed.

1. Introduction

The development of tidal stream energy extraction technology and the establishment of a tidal stream industry has seen considerable growth in the past two decades (Neill et al., 2017). As the tidal stream industry is only just starting to take the first steps moving from testing full-scale prototypes toward commercially viability, strategic planning of the marine environment is needed to maximise its full potential (Renewable UK, 2015). Many of the high velocity sites suitable for energy extraction are in close proximity and therefore could potentially interact significantly with one another. It is not efficient or in the best interest of the industry to consider each project in isolation. Cumulative impact assessments should be conducted, but have only recently been considered (Fairley et al., 2015; Wilson et al., 2012). Wilson et al. (2012) investigated the interaction between energy extraction from tidal stream and tidal barrages across the UK and its effect on the European continental shelf. Results showed severe near-field effects if tidal stream extraction is not limited and would require close management between nearby projects to limit environmental and economic impacts (Wilson et al., 2012).

Whilst a lot of focus has been given to modelling the Pentland Firth

(Martin-Short et al., 2015; Draper et al., 2014; Woolf, 2013), it is not the only site being developed within the UK; the Irish Sea also has a number of proposed developments. The Irish Sea has long been studied (Robinson, 1979; Pingree and Griffiths, 1987; Davies and Jones, 1992; Young et al., 2000). Depths in the Irish Sea range from intertidal mud flats to ~140 m in the central Irish Sea, to the extreme of 250 m in the North Channel. Two amphidromic systems are found in the Irish Sea, one on the east coast of Ireland and one to the north of Northern Ireland. Tidal ranges in the east Irish Sea are the largest in the UK, with ranges more than 9 m at Workington and 12 m at Hinkley (British Oceanographic Data Centre). Large tidal velocities (> 2 m/s) can be found in several locations in the Irish Sea, notably around Pembrokeshire, Anglesey and Northern Ireland (Robins et al., 2015).

Several studies have been conducted assessing these locations for the available tidal energy resource and the suitability for tidal stream extraction (Robins et al., 2015; Lewis et al., 2015; Neill et al., 2014). However, these studies do not include the presence of tidal stream devices, nor the interaction of devices or arrays of devices with one another. Robins et al. (2015) investigate how the ratio of the M2 and S2 harmonics can affect the annual practical power and estimate the spatial distribution of a tidal stream capacity factor. Whilst an annual

Please cite this article as: Haverson, D., Ocean Engineering (2017), http://dx.doi.org/10.1016/j.oceaneng.2017.04.003

power production is calculated for two sites, the Pentland Firth and Alderney, *"power extraction from individual turbines has not been simulated"* and *"neglect any device feedbacks"*. Lewis et al. (2015) investigate the total annual mean tidal resource of the Irish Sea within the constraints of 1st generation devices (velocities > 2.5 m/s and depths between 25 and 50 m) and show that the total potential resource could be larger if devices could be deployed in water depths greater than 50 m. Neill et al. (2014) investigate the phasing of tidal sites around the European shelf for power generation, but conclude there is minimal phase diversity between sites for power generation.

As well as the discussed resource assessments, studies have been conducted in the Irish Sea including the presence of tidal turbines. Robins et al. (2014) assessed the impact of tidal-stream arrays in relation to the natural variability of sedimentary processes at Anglesey, but only included a single tidal array of increasing capacity. Hashemi et al. (2015) investigated the influence of waves on tidal resource at Anglesey, showing that extreme wave-current interactions can reduce the tidal resource by 20%. Walkington & Burrows (2009) conducted an assessment of tidal stream power at multiple sites. However, the hydrodynamic effect of the tidal array at each of the four locations was considered in isolation. Furthermore, the tidal turbines were represented as a constant drag term, neglecting the operation of the turbine and the drag due to the support structure, leading to an under-representation of the total force and influence exerted by the turbine.

At the time of this study, there were eight existing and proposed tidal projects within the Irish Sea, totalling 264 MW. These include: Ramsey Sound (10 MW), Anglesey (10 MW), Strangford Loch (1.2 MW), Mull of Kintyre (3 MW), Torr Head (100 MW), Fair Head (100 MW), Sound of Islay (10 MW) and West of Islay (30 MW) (see

Fig. 1). The size of these arrays represent the actual proposed installed capacities of the site developers and not the maximum theoretical capacities of the sites. Wilson et al. (2012) have previously investigated the interaction of extreme future large scale deployments (> 85 GW by 2050). The aim of this study is to investigate the interaction of actual projects detailed by site developers. Since this work has been undertaken, funding for the Anglesey project was removed and the project stalled. However, for the purpose of this analysis, it has been retained. This paper will investigate the cumulative impact of tidal energy in the Irish Sea to examine the extent to which the projects interact with each other. For this study, only tidal stream developments have been considered; tidal barrages were not included.

2. Irish Sea model

A high-resolution depth-averaged model of the Irish Sea was built using an unstructured triangular mesh, with the hydrodynamic software Telemac2D (v7p1) (Telemac). The model domain extends between 50.14°N–56.72°N and 2.38°W–7.73°W and is shown in Fig. 1. The unstructured mesh was discretised with 305,000 nodes, and has a resolution of 15 km around the open boundary, reducing to 1 km along the coastline. Bathymetry of the area, relative to Chart Datum, was sourced from the Department for Environment, Food & Rural Affair's UKSeaMap 2010 and was provided by the Centre for Environment, Fisheries and Aquaculture Sciences. The resolution of the bathymetry points from this dataset are 1 arc-second (~30 m). The bathymetry was corrected to Mean Sea Level by applying the maximum tidal range to the depths. As bathymetry strongly influences hydrodynamic characteristics, a high resolution 2 m and 4 m resolution bathymetry, from
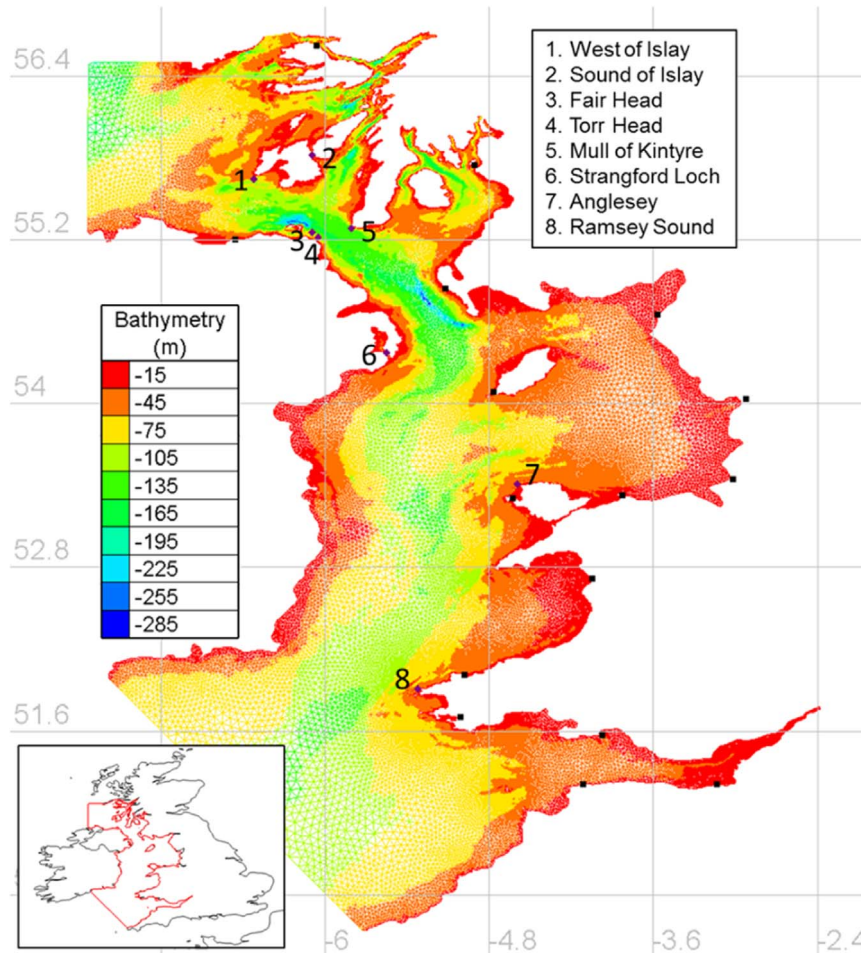

Fig. 1. Irish Sea model domain showing the locations of the tidal arrays (purple diamonds) and tide gauge locations (black squares) used for validation.

Table 1
Characteristics of the five device technologies used to parameterise the turbines in the model.

Device	Rate Power (MW)	Rotor Diameter (m)		Hub Height (m)	Monopile Diameter (m)	U_C (m/s)	U_D (m/s)	C_{T0}	C_{P0}
Delta stream	1.2	18	15		2	0.8	2.25	0.81	0.27
SeaGen-S	2	20	15		2	0.8	2.5	0.8	0.41
Openhydro	2	16	16		2	0.8	3.5	0.8	0.45
Hammerfest	1	23	22		2	0.8	2.5	0.7	0.33
Nautricity	0.5	14	12		0	0.8	2.5	0.8	0.41

the UK Hydrographic Office (UKHO), has also been applied around Ramsey Sound, Fair Head, Torr Head and the Sound of Islay. The hydrodynamics are forced along the open boundaries using tidal constituents from the OSU TPXO European Shelf 1/30° regional model (OSU Tidal Data Inversion). As both prescribed elevations and velocities are applied at the boundary, the open boundaries are set far from the area of interest to reduce any dampening on the far field effects of a tidal array. The model uses a k-ε turbulence model. The depth-averaged parameterisation of k-ε in Telemac was developed by Rastogi and Rodi (1978) with the velocity diffusivity set to 1×10−06 m^2/s, representing the kinematic viscosity of water. The Nikuradse law for bottom friction was used, with a constant value of k_s =0.04 applied to the whole model domain.

3. Modelling tidal turbines

The effect of a tidal array is introduced into the model as an extra sink in the momentum equations. This has become the common method for modelling tidal turbines (Robins et al., 2014; Ahmadian et al., 2012; Neill et al., 2012). An individual tidal turbine causes a change in momentum in two parts: a thrust force produced by the rotor due to energy extraction and a drag force caused by the supporting structure, i.e.-

$$F_D = \frac{1}{2}\rho C_T A_r U^2 + \frac{1}{2}\rho C_D A_s U^2, \qquad (1)$$

where U is the upstream velocity, ρ is the density of sea water, C_T is the thrust coefficient, C_D is the drag coefficient, A_r is the swept area of the rotor and A_s is the frontal area of the support structure. The operation and output of the turbine is controlled by the pitch of the rotor blades, resulting in changes in the thrust and power coefficient. The methodology used to represent the operation of the tidal turbines is presented by Plew & Stevens (2013). Below the cut-in speed the rotor produces no power, meaning the thrust and power coefficient are zero, i.e. C_T = C_P =0. Between the cut-in speed U_C and the rated speed U_D it is assumed the pitch of the rotor blade is fixed along with the tip speed ratio, resulting in a constant thrust and power coefficient C_{T0} and C_{P0}. Above the rated speed the pitch of the rotor blade is increased to reduce the power produced and maintaining rated power P_D. The power coefficient is parameterised as:

$$C_P = \frac{2P_D}{\rho A_r U^3}, \qquad U > U_D, \qquad (2)$$

For simplicity, Plew and Stevens assume a fixed relationship between the thrust and power coefficient, resulting in the thrust coefficient above rated speed being parameterised as:

$$C_T = \frac{C_{T0}}{C_{P0}} \frac{2P_D}{\rho A_r U^3}, \qquad U > U_D \qquad (3)$$

The resolutions of unstructured meshes are typically larger than the modelled turbines, therefore, the drag force is spread over the area of several elements. An unstructured mesh can result in elements of different sizes, thus a different force may be applied to different elements within the same area defined as one turbine. Therefore, a

regular mesh using triangular elements is used in the area where turbines are modelled, ensuring any variation is due to the hydrodynamics and not the mesh. The resolution of these regular meshes is 20 m. Each device is represented individually, with the force of each device spread over eight elements. For Ramsey Sound and Sound of Islay, the array layout is set as detailed by the site developer. The single turbine within Strangford Loch is positioned as deployed. For the remaining site, each array is made up of rows that stretch the permittable width of the site, with a lateral spacing between devices of two and half rotor diameters (EMEC, 2009). For arrays with multiple rows, the devices are ten rotor diameters downstream of each other (EMEC, 2009) in a staggered formation (Couch and Bryden, 2007).

Over the eight tidal developments, five different tidal technologies have been proposed. Ramsey Sound will use Delta Stream devices; Strangford Loch, Anglesey, West of Islay and Fair Head will use Atlantis Resource's MCT SeaGen-S; Torr Head will use Openhydro; Sound of Islay will use Hammerfest and Mull of Kintyre will use Nautricity. For all the projects, each device is modelled individually. Furthermore, each technology type is parameterised differently in the model. The turbine parameters for each device can be found in Table 1. As the SeaGen-S, Nautricity and Delta Stream device have multiple rotors, the total force of these devices is combined into one device. For simplicity, all the support structures have been assumed to be single cylindrical monopiles, with the exception of Openhydro and Nautricity. Openhydro has two monopoles and Nautricity is a tethered floating turbine. The drag coefficient for the cylindrical monopile was C_D=0.9. The drag of the tether has been ignored due to its negligible drag force.

4. Validation

4.1. Free surface elevations

Validation data has been obtained from the British Oceanographic Data Centre (BODC) (British Oceanographic Data Centre) for surface elevation at sixteen tide gauges, whose locations are shown in Fig. 1. After a 5 day spin-up period, the model was run for 30 days from 17/05/2012 00:00 to 16/06/2012 00:00. Comparisons of the modelled free surface elevation and observed tidal elevations at each tide gauge are shown in Fig. 2.

The results in Fig. 2 illustrate the validation between modelled and observed values, and show these are in close agreement at the tide gauges in the southern half of the model (Fishguard, Milford Haven, Mumbles, Ilfracombe and Hinkley) which includes the Severn Estuary. Tide gauges in the central Irish Sea, such as Barmouth, Millport, Portpatrick and Port Erin show a larger scattering due to a phase misalignment. This is due to features, e.g. River Clyde, Afon Mawddach and Lough Foyle, being clipped from the model to improve computational efficiency. Portrush shows some disagreement, however, this may be more due to errors in the tide gauge rather than the model, as a number of erroneous records were removed from the tide gauge data.

To validate the free surface elevations, three statistical quantities have been used: the coefficient of determination, the root mean squared error and the scatter index. The coefficient of determination, R2, is the proportion of the variance explained by a linear regression model predicting
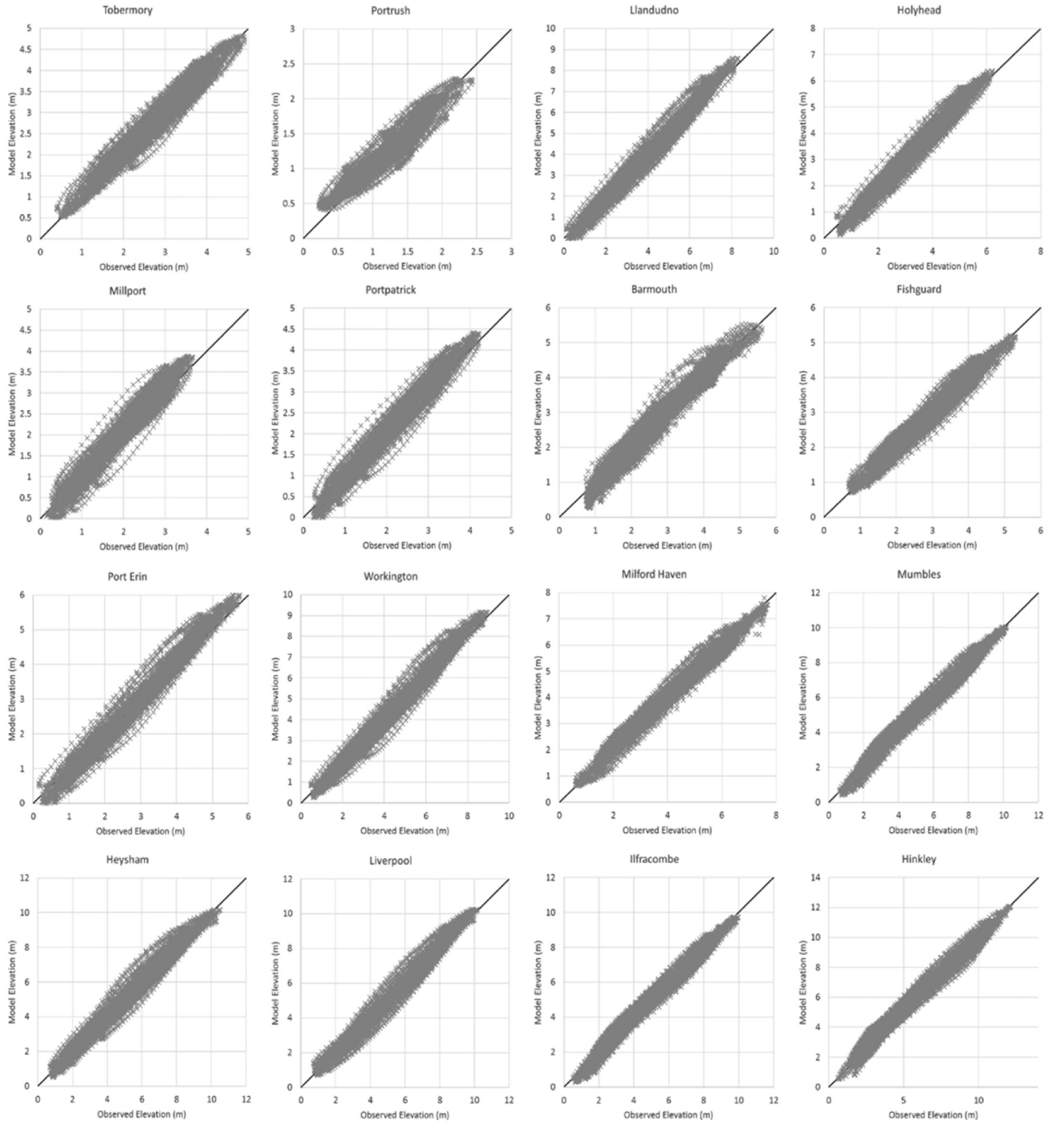
Fig. 2. Comparison of observed and modelled free surface elevation. The black line represents a y=x relationship with the dashed line representing a regression line of best fit.

the dependant variable from the independent variable as is defined as:

$$1 - \frac{\sum_i (y_i - \bar{y}_i)^2}{\sum_i (\hat{y}_i - \bar{y}_i)^2} \tag{4}$$

where y_i are the observed values, $\bar{y}_i$ is the mean of the observed values and $\hat{y}_i$ are the predicted values. The value of R^2 ranges between 0 and 1, with 0 representing no correlation between predicted and observed values and 1 representing a perfect correlation. The root mean squared error (RMSE) is the standard deviation of error between the observed and predicted values and is defined as:

$$\sqrt{\frac{1}{n} \sum_{i=1}^{n} (\hat{y}_i - y_i)^2} \tag{5}$$

where n is the total number of observations. The scatter index is RMSE normalised by the mean of the observations:

$$\frac{RMSE}{\bar{y}_i} \times 100\% \tag{6}$$

Table 2 summarises the validation statistics of the sixteen tide gauges.

4

Table 2
Validation statistics of the 16 tide gauges.

Tide Gauge	R^2	RMSE (m)	Scatter Index (%)
Tobermory	0.965	0.200	7.54
Portrush	0.901	0.149	5.64
Millport	0.950	0.260	9.83
Portpatrick	0.969	0.235	8.88
Port Erin	0.974	0.301	11.35
Workington	0.977	0.381	14.38
Heysham	0.974	0.407	15.36
Liverpool	0.974	0.403	15.19
Llandudno	0.976	0.387	14.58
Holyhead	0.968	0.308	11.63
Barmouth	0.948	0.287	10.82
Fishguard	0.952	0.236	8.89
Milford Haven	0.974	0.280	10.56
Mumbles	0.978	0.368	13.87
Illfracombe	0.977	0.363	13.67
Hinkley	0.975	0.506	19.07

The coefficient of determination shows that there is a good correlation between the observed and modelled free surface. However, the RMSE and scatter index indicate a poorer correlation. As the free surface varies about the mean sea level, the difference between the mean of the observed and the predicted will always be small. The difference between time series are more likely to be due to uncertainty in the location of the tide gauges than an error in the model (Gunn and Stock-Williams, 2013).

4.2. Harmonic analysis

The model was run for 30 days to provide a time series of sufficient length to permit a harmonic analysis which includes the dominant components. The dominant components are the M2 and S2 constituents. Tables 3 and 4 show the comparison between harmonic constituents from the UKHO and the model for the M2 and S2 constituents for tidal elevations. Fig. 3 plots the comparison between the modelled and observed M2 & S2 constituent amplitude for tidal elevations.

Analysis of the harmonics reveals agreement between the model and observations in the northern and southern parts of the model domain. In the central Irish Sea, the model over-predicts the elevations, on average, by 13%. Pingree & Griffith (1979) found a similar

effect in their model of the Irish Sea. Whilst they found an improvement by increasing the drag coefficient in this region they could not remove all the discrepancies due to errors caused by a depth-averaged model. However, the validation of this model is comparable to other studies of the Irish Sea (Robins et al., 2015; Lewis et al., 2015). Table 5 summarises the model validation compared against Robins et al. (2015) and Lewis et al. (2015) with this study. Compared to the tide gauges the scatter index is smaller and within acceptable ranges, 7.44% and 6.93% for the M2 and S2 respectively.

Along with tidal elevations, a harmonic analysis was performed on the tidal currents. Currents have been validated against published tidal current ellipse data from 31 offshore current meters (see (Young et al., 2000) and (Jones, 1983) for further details). Fig. 4 plots the comparison between the modelled and observed M2 & S2 constituent amplitude for tidal currents.

Analysis of the harmonics reveals agreement between the model and observations. It can be seen that the model does slightly overestimate the currents, with a bias towards the model of 3.4 cm/s for M2 and 2.4 cm/s for S2. However, the validation of this model is comparable to other studies of the Irish Sea (Robins et al., 2015; Lewis et al., 2015). Table 6 summarises the model validation compared against Robins et al. (2015) and Lewis et al. (2015) with this study.

5. Results–Irish Sea model

To determine if any of the tidal projects were interacting with each other, their zones of influence were calculated using the normalised range of difference. The model is run twice: a base case (without turbines) and a turbine case (with all turbines). The range of difference is calculated by subtracting the magnitude of velocity at each node of the mesh of the turbine run from the magnitude of the velocity in the base case. This is done for each time step, producing a temporally and spatially varying difference between the two models. The range of difference is the difference between the maximum increase and decrease at each node over the whole model run. The range is then normalised to the maximum change to give a percentage figure. The range of difference does not represent the instantaneous velocity reduction due to the direct wake of the turbine array at any one time. Instead, it gives an indication of the total temporal and spatial extent of change. Fig. 5 shows the cumulative normalised range of difference for the eight developments over the 30-day model run.

The normalised range of difference from Ramsey Sound (10 MW), the Anglesey Skerries (10 MW), Strangford Loch (1.2 MW), West of

Table 3
Comparison between observed and modelled M2 constituent for tidal elevations.

Tide Gauge	M2					
	Observed Amplitude	Model Amplitude	Percentage Difference	Observed Phase	Model Phase	Percentage Difference
	(m)	(m)	(%)	(deg)	(deg)	(%)
Tobermory	1.27	1.29	1.6	175.0	168.1	−1.9
Port Ellen	0.15	0.17	13.3	50.3	52.2	0.5
Portrush	0.54	0.50	−7.4	201.0	203.9	0.8
Millport	1.12	1.30	16.1	341.0	341.3	0.1
Portpatrick	1.33	1.54	15.8	331.0	330.8	−0.1
Port Erin	1.88	2.08	10.7	322.7	321.2	−0.4
Workington	2.70	3.00	11.2	333.7	330.5	−0.9
Heysham	3.18	3.24	1.9	325.0	321.7	−0.9
Liverpool	3.08	3.16	2.6	315.2	318.6	1.0
Llandudno	2.65	2.96	11.8	310.1	310.3	0.1
Holyhead	1.80	2.03	12.8	292.0	294.3	0.6
Barmouth	1.47	1.52	3.4	244.0	241.5	−0.7
Fishguard	1.37	1.32	−3.6	208.0	212.2	1.2
Milford Haven	2.22	2.19	−1.4	173.0	172.6	−0.1
Mumbles	3.18	3.10	−2.5	171.0	171.6	0.2
Ilfracombe	3.07	3.03	−1.3	163.0	162.3	−0.2
Hinkley	3.80	3.90	2.6	185.0	181.5	−1.0

Table 4
Comparison between observed and modelled S2 constituents for tidal elevations.

Tide Gauge	S2					
	Observed Amplitude	Model Amplitude	Percentage Difference	Observed Phase	Model Phase	Percentage Difference
	(m)	(m)	(%)	(deg)	(deg)	(%)
Tobermory	0.52	0.54	3.8	211.0	204.4	−1.8
Port Ellen	0.16	0.13	−18.8	141.0	143.9	0.8
Portrush	0.23	0.22	−4.3	216.0	212.7	−0.9
Millport	0.30	0.34	13.3	33.0	31.9	−0.3
Portpatrick	0.37	0.43	15.8	16.0	15.0	−0.3
Port Erin	0.56	0.63	12.3	2.9	1.3	−0.4
Workington	0.86	0.95	11.0	17.3	13.6	−1.0
Heysham	1.03	1.04	1.0	8.0	4.1	−1.1
Liverpool	1.00	0.99	−1.0	359.2	361.7	0.7
Llandudno	0.86	0.95	10.2	352.7	351.5	−0.3
Holyhead	0.59	0.65	11.0	329.0	332.3	0.9
Barmouth	0.53	0.57	7.5	283.0	279.8	−0.9
Fishguard	0.54	0.50	−7.4	249.0	253.2	1.2
Milford Haven	0.81	0.78	−3.7	218.0	217.0	−0.3
Mumbles	1.12	1.10	−1.8	221.0	218.2	−0.8
Ilfracombe	1.12	1.08	−3.6	209.0	208.3	−0.2
Hinkley	1.42	1.37	−3.5	237.0	232.5	−1.3

Islay (30 MW) and the Sound of Islay (10 MW) are sufficiently small that their zones of influence do not overlap. However, Fair Head and Torr Head do overlap. The zone of influence for Mull of Kintyre is large given the scale of project (3 MW), especially when compared to Fair Head (100 MW) and Torr Head (100 MW). Fair Head and Torr Head may be influencing the Mull of Kintyre as well.

6. Northern Ireland model

As the model domain is computationally expensive to run, a smaller model domain encompassing these three projects was created to further investigate the interaction. The Northern Ireland model uses the same structure as the full Irish Sea model but only covers the smaller area of interest. It uses the same coastline and bathymetry as the previous model. The model domain extends between 54.80°N–56.02°N and 4.62°W–7.04°W and is shown in Fig. 6. The unstructured mesh was discretised with 137,000 nodes. A regular mesh using triangular elements is used in the area where turbines are modelled. The resolution of the regular mesh is 20 m.

The model was run over the same period of time as the Irish Sea model.

After a 5-day spin-up period, the model base case was run for 30 days to allow enough time to include a sufficient number of harmonic components in the analysis. Harmonic constituents at ten locations (see Fig. 6) were extracted from the TPXO database to validate the model. Tables 7 and 8 show the comparison between harmonic constituents from the TPXO database and the model for the M2 and S2 constituents. Fig. 7 shows the comparison between the modelled and observed M2 and S2 constituent amplitude.

Results show the Northern Ireland model validates better than the Irish Sea domain. The RMSE of the M2 and S2 amplitude is 4 cm and 2 cm, respectively, with a scatter index of 7.55% and 3.62%. However, this may be due to the model being validated using harmonics from the same database that drives the model. As the Irish Sea model was validated against tide gauge data, the harmonics from the Northern Ireland model were also compared against the harmonics of the Irish Sea model at the ten locations. The M2 amplitude of the Northern Ireland model is on average 4 cm smaller than the Irish Sea model. The
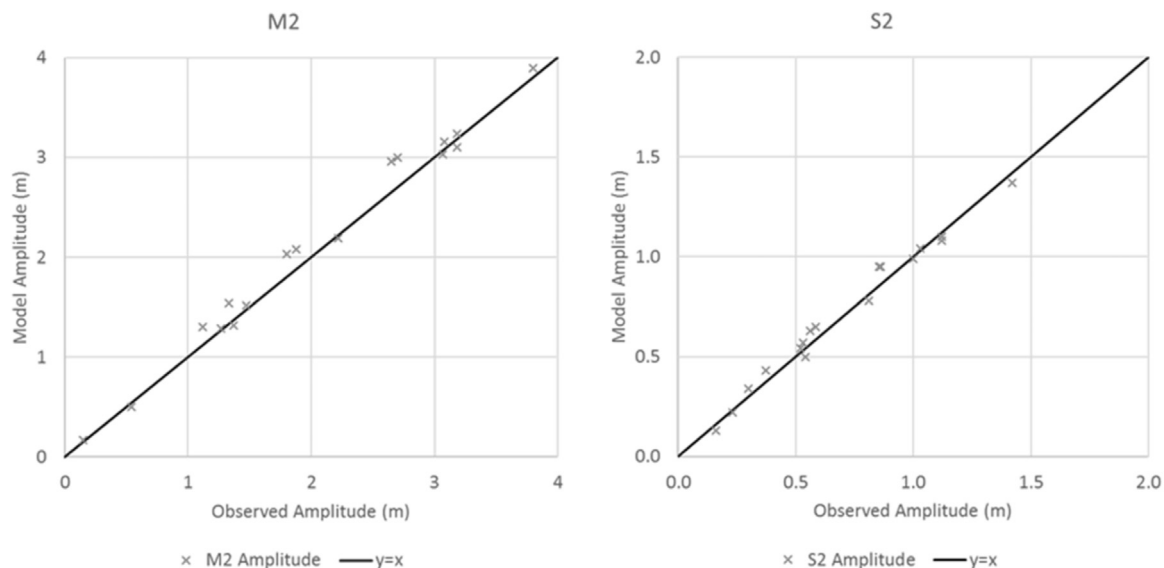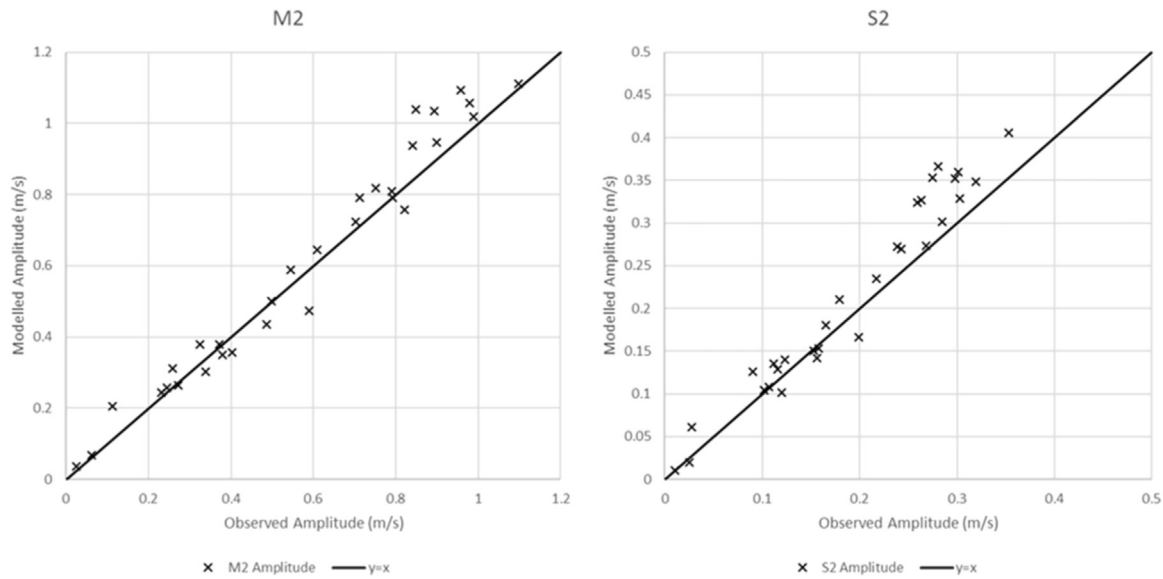

Fig. 3. Comparison between modelled and observed M2 (left) and S2 (right) tidal constituent for tidal elevations.

Table 5
Comparison of model validation of tidal elevations with similar studies.

RMSE	Present Study		Robins et al. (2015)		Lewis (2015)	
	Amplitude (cm)	Phase (deg)	Amplitude (cm)	Phase (deg)	Amplitude (cm)	Phase (deg)
M_2	15	3	15	12	13	6
S_2	5	3	5	10	8	14

Fig. 4. Comparison between modelled and observed M2 (left) and S2 (right) tidal constituent for tidal velocities.

Table 6
Comparison of model validation of tidal currents with similar studies.

RMSE	Present Study Amplitude	Robins et al. (2015) Amplitude	Lewis (2015) Amplitude
	(cm/s)	(cm/s)	(cm/s)
M_2	6.7	4.6	8
S_2	3.7	1.6	2

S2 amplitude is on average 2 cm smaller. The Irish Sea model was found to be slightly over predicting the amplitude of the M2 and S2 constituent, meaning that the smaller amplitudes in the Northern Ireland model show an improvement. As the model shows close agreement to both the TPXO database and the Irish Sea model, the validation of Northern Ireland model will be considered adequate for this study.

As insufficient points from the previous harmonic analysis lie within the smaller model domain, current observations were obtained from the BODC (British Oceanographic Data Centre). The two validation points lie to the east and west of the sites of interest and are shown in Fig. 6. The first observation point was located at 55.46ºN and 6.2333ºW and recorded tidal velocities between 13-09-1994 16:25 and 29-10-1994 08:35, with a ten-minute interval. The second observation point was located 55.1167ºN and 5.8883ºW and recorded tidal velocities between 08-05-1995 12:15 and 08-06-1995 08:35, with a ten-minute interval. As the period of observation does not match the period of the model, a direct comparison cannot be made. However, it can be seen in Fig. 8, that both the shape and magnitude of the tidal velocities are in good agreement.
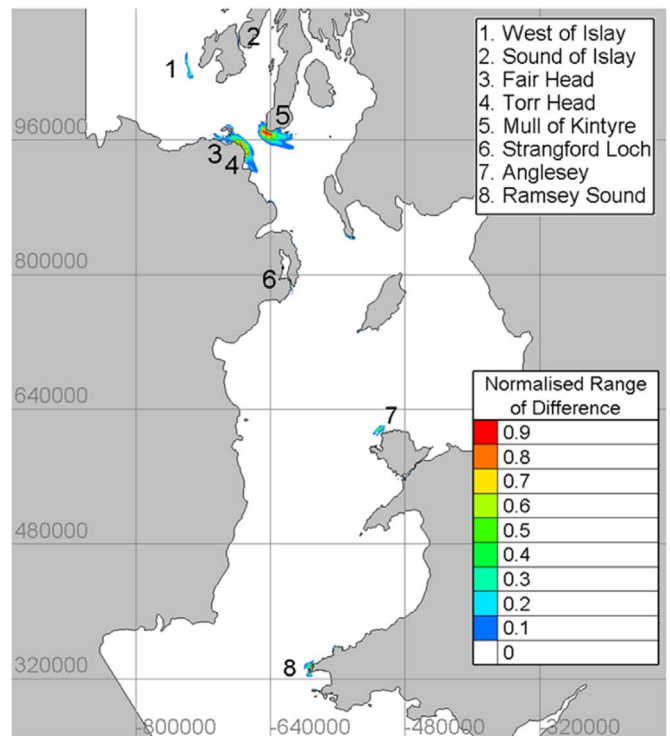

Fig. 5. The cumulative zones of influence for all eight tidal projects, calculated using the range of difference.

7. Results–Northern Ireland model

The base case was run for 30 days to allow for a harmonic analysis for validating the model. The model runs containing the tidal turbines
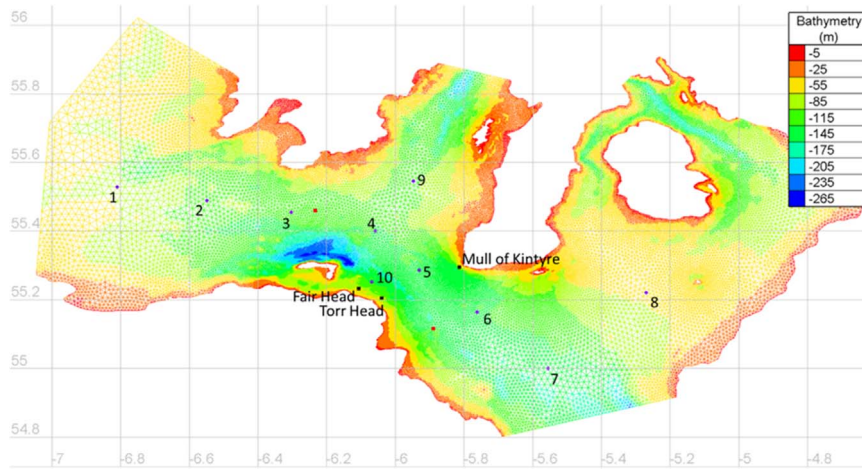
Fig. 6. Northern Ireland model domain. Locations of the tidal arrays are indicated in black dots, the tidal elevation validation points in purple diamonds and current observations in red squares.

were limited to the first 10 days, after the 5-day spin-up. This period encompasses the peak spring tidal velocities. Fig. 9 shows the zone of influence for case 8 (all three projects within the Northern Ireland model), case 2 (only Fair Head), case 3 (only Torr Head), and case 5 (Fair Head and Torr Head).

In Fig. 9-a, the zone of influence around Fair Head and Torr Head extends to a range of approximately 75 km. In comparison, the zone of influence around Mull of Kintyre is approximately 20 km. This is larger than expected given Mull of Kintyre is using relatively small 500 kW devices. The presence of Fair Head and Torr Head systems running together lead to impact off the Mull of Kintyre coastline, regardless of the presence of the 3 MW tidal development, as seen in Fig. 9-b, c & d. Results indicate that Fair Head is having a larger impact than Torr Head and the spatial extent of change due to Fair Head alone is similar to the spatial extent where all three projects are modelled together. The true influence of Fair Head can be seen more clearly from the energy production. Table 9 shows the energy produced over the 10-day period. Table 10 shows the percentage difference in energy production.

From the energy production it can be seen that the interaction between Mull of Kintyre and the other projects is an order of magnitude smaller than the interaction between Fair Head and Torr Head. The Mull of Kintyre project benefits in all cases with the inclusion of Fair Head and Torr Head. Torr Head loses the most energy in this study. The total energy production at Fair Head is reduced by over 2% due to Torr Head, whereas, Torr Head itself loses 17% due to the presence of Fair Head.

Table 8
Comparison between observed and modelled S2 constituent.

Location	S2					
	Observed Amplitude	Model Amplitude	Difference	Observed Phase	Model Phase	Difference
	(m)	(m)	(m)	(deg)	(deg)	(deg)
1	0.30	0.26	−0.03	194.9	194.4	−0.5
2	0.22	0.19	−0.03	189.3	185.0	−4.3
3	0.12	0.10	−0.02	178.2	176.5	−1.7
4	0.05	0.04	−0.01	161.0	133.1	−27.8
5	0.05	0.06	0.01	28.4	29.9	1.6
6	0.17	0.15	−0.02	15.5	16.6	1.1
7	0.25	0.24	−0.01	9.4	10.3	0.9
8	0.27	0.26	0.00	22.2	24.1	1.9
9	0.08	0.08	0.00	136.3	121.4	−14.9
10	0.04	0.04	−0.01	306.4	314.4	8.0

8. Discussion

The difference in energy production between Fair Head and Torr Head is caused by a large tidal asymmetry between the flood and the ebb tide. The flood (west to east) is considerably stronger than the ebb (east to west) and can clearly be seen in the power production. Fig. 10 shows the total instantaneous power production for Fair Head and Torr Head for cases 2, 3 and 5 (both arrays operating separately and operating concurrently).
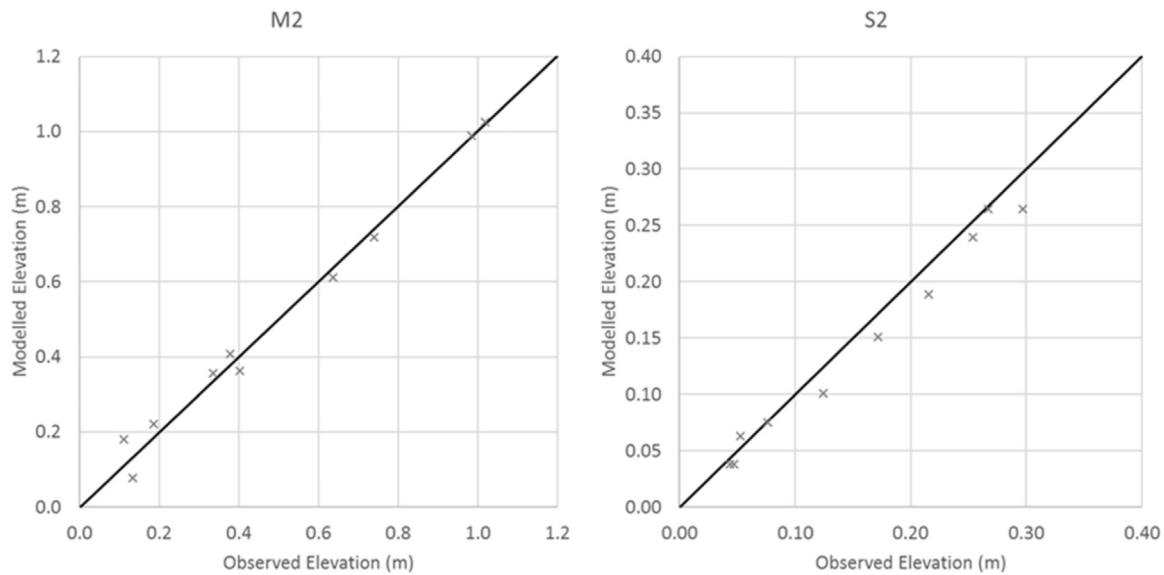
Table 7
Comparison between observed and modelled M2 constituent.

Location	M2					
	Observed Amplitude	Model Amplitude	Difference	Observed Phase	Model Phase	Difference
	(m)	(m)	(m)	(deg)	(deg)	(deg)
1	0.64	0.61	−0.03	164.2	164.0	−0.1
2	0.40	0.36	−0.04	158.1	154.9	−3.2
3	0.13	0.08	−0.06	137.9	145.4	7.5
4	0.11	0.18	0.07	344.9	338.3	−6.6
5	0.38	0.41	0.03	332.3	330.2	−2.2
6	0.74	0.72	−0.02	331.7	329.0	−2.7
7	0.98	0.99	0.01	327.8	326.5	−1.2
8	1.02	1.03	0.01	338.9	337.6	−1.3
9	0.18	0.22	0.04	28.5	15.0	−13.6
10	0.33	0.36	0.02	300.8	301.7	0.9

Fig. 7. Comparison between modelled and observed M2 (left) and S2 (right) tidal constituent.

When both arrays operate separately, the power production is approximately 4–5 times larger on the flood tide than the ebb tide. As Fair Head is situated to the west of Torr Head, the tidal asymmetry means that Fair Head has a larger detrimental effect on Torr Head. During the flood tide, Fair Head extracts energy from the flow reducing the peak velocities at Torr Head such that the power production at Torr Head is reduced to approximately two thirds the power output as if it was operating in isolation. Whereas, during an ebb tide when the flow is slower, the presence of Torr Head only reduces the power output at Fair Head by 20%. Despite both arrays having an installed capacity of 100 MW, when operated in isolation, Fair Head never exceeds 40 MW on the ebb and Torr Head never exceeds 30 MW. Furthermore, due to the intra-array effects, the total maximum power output is 97.8 MW for Fair Head and 93.8 MW for Torr Head, when operated separately. When the two sites are operated concurrently, the maximum power during the flood tide is 98.1 MW for Fair Head and 64.5 MW for Torr Head. This represents a 31% reduction in peak power output. This is considerably more than when considering the reduction in tidal resource from wave-current interactions. The inclusion of waves can reduce the tidal resource by 20% in extreme conditions and by 15% in

winter mean conditions (Hashemi et al., 2015). The proximity and position of the two tidal sites mean they will share similar wave resources, meaning a reduction in resource will affect both sites. By reducing tidal currents, the impact of Fair Head would reduce during the flood, increasing the power output at Torr Head. However, extreme conditions only affect a small portion of the year, meaning the impact on the annual energy production is still present. Further work would be required to quantify the effect wave-current interaction at this study location.

Maximising the power output within in the constraint of the Levelised Cost of Energy of a tidal project is considered best single outcome for optimising the cumulative deployment of tidal stream energy extraction (Wilson et al., 2012). But, it should also be considered in partnership with the constraint of minimising the environmental impact. The economic viability of tidal energy is not considered within this study. It is clear that with a 17% reduction in energy production, if deployed alongside Fair Head, Torr Head would lose a considerable amount of revenue. However, if Torr Head could still operate commercially despite the presence of Fair Head then there are environmental positives. Comparing the zones of influence in Fig. 9
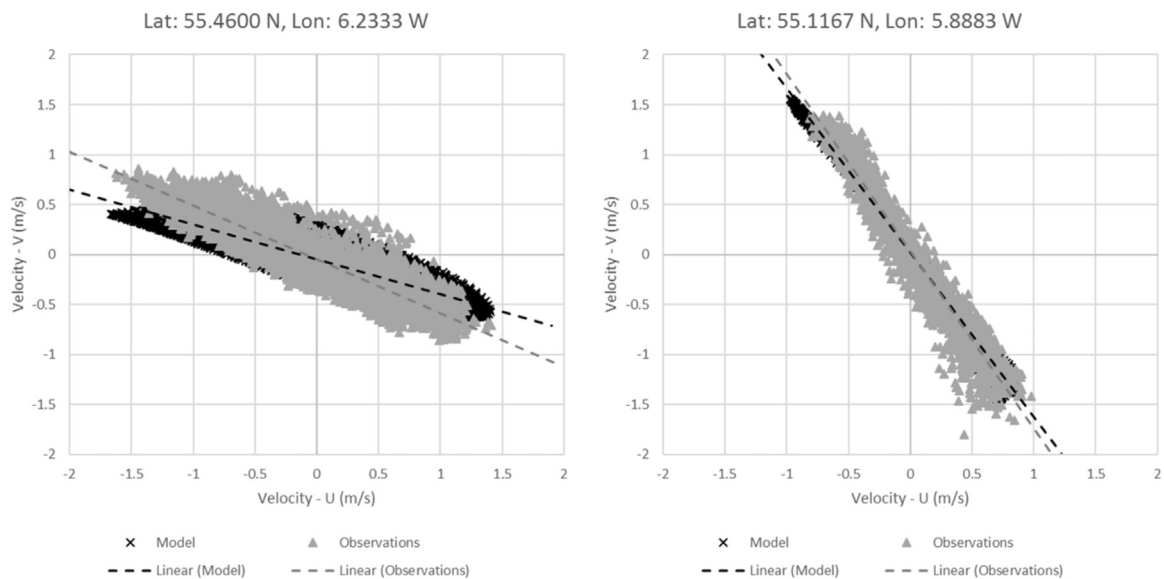

Fig. 8. Comparison between modelled and observed tidal velocities at 55.46°N, 6.2333°W and 55.1167°N, 5.8883°W.
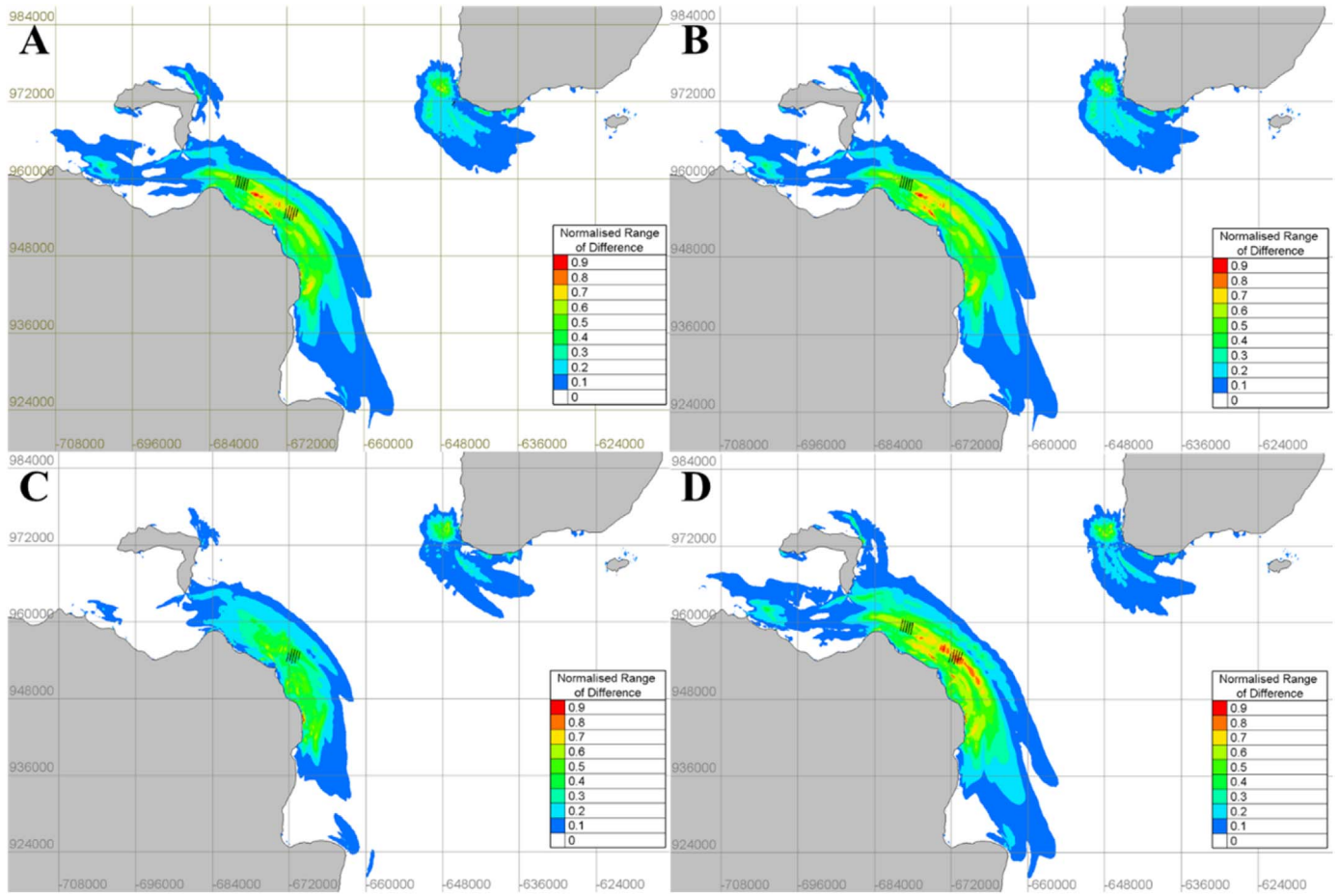
Fig. 9. Cumulative zone of influence for A) case 8 (all three projects), B) case 2 (only Fair Head), C) case 3 (only Torr Head) and D) case 5 (Fair Head and Torr Head).

Table 9
Energy production of each tidal project for all eight test cases.

Case	Fair Head (MWh)	Torr Head (MWh)	Mull of Kintyre (MWh)
1	–	–	–
2	4942.0	–	–
3	–	4179.4	–
4	–	–	423.2
5	4828.6	3470.9	–
6	4934.7	–	423.6
7	–	4155.4	423.4
8	4817.1	3464.8	423.6

Table 10
Percentage change in energy production for Cases 5 – 8.

Case	% Difference		
	Fair Head	Torr Head	Mull of Kintyre
5	−2.29	−16.95	–
6	−0.15	–	0.09
7	–	−0.57	0.05
8	−2.53	−17.10	0.09

the spatial extent of change is similar. If Fair Head is built, then the additional impact of Torr Head is reduced. Other impacts should also be considered. Hydrodynamics are a primary driver in physical processes, such as suspended sediments, sediment transport and substrate composition. A more accurate predictor of the impact on physical processes would be the changes to mean and maximum bed

shear stress as this can give a perspective of change over a longer timescale. Bed shear stress is calculated as:

$$\tau = \rho \, C_d \|\mathbf{u}\| \mathbf{u}. \tag{7}$$

where ρ is the density of seawater, C_d is the bottom drag coefficient and $\|\mathbf{u}\|$ is the magnitude of the velocity vector. For the purpose of calculating bed shear stress, the value $C_d = 0.0025$ was used. Fig. 11 shows the maximum and mean change in bed shear stress for case 8 (all three projects).Case 8 represents the worst case scenario with all three projects present. Whilst a change could be seen around the Mull of Kintyre in Fig. 9, the impact on the mean and maximum bed shear stress is minimal. The major change is limited to the vicinity of Fair Head and Torr Head. For case 8, the peak reduction in maximum bed shear stress is 23.2 Pa. The peak reduction in mean bed shear stress is 2.6 Pa. These values are similar to changes seen in the Pentland Firth, as modelled in (Martin-Short et al., 2015). When only Fair Head is present the peak reduction in maximum and mean bed shear stress is 17.5 Pa and 2.4 Pa respectively. Fig. 12 show the maximum and mean change in bed shear stress for case 2. The black contour represents the extent of change for case 8, as shown in Fig. 11.

The spatial extent between case 2 and case 8 is very similar. In both cases sediment would accumulate within the vicinity of the arrays with areas of erosion either side. The turbines are located in areas that are void of any fine sediment and are mainly gravel or exposed bed rock (Tidal Ventures, 2015). The magnitude of change would result in medium gravel accumulating in an area of coarse gravel so the impact is likely to be minimal. This change would occur within the Torr Head site with or without the presence of Torr Head if Fair Head was present. Sand is present between the coastline and the tidal turbines and the resulting increase in bed shear stress would likely cause erosion
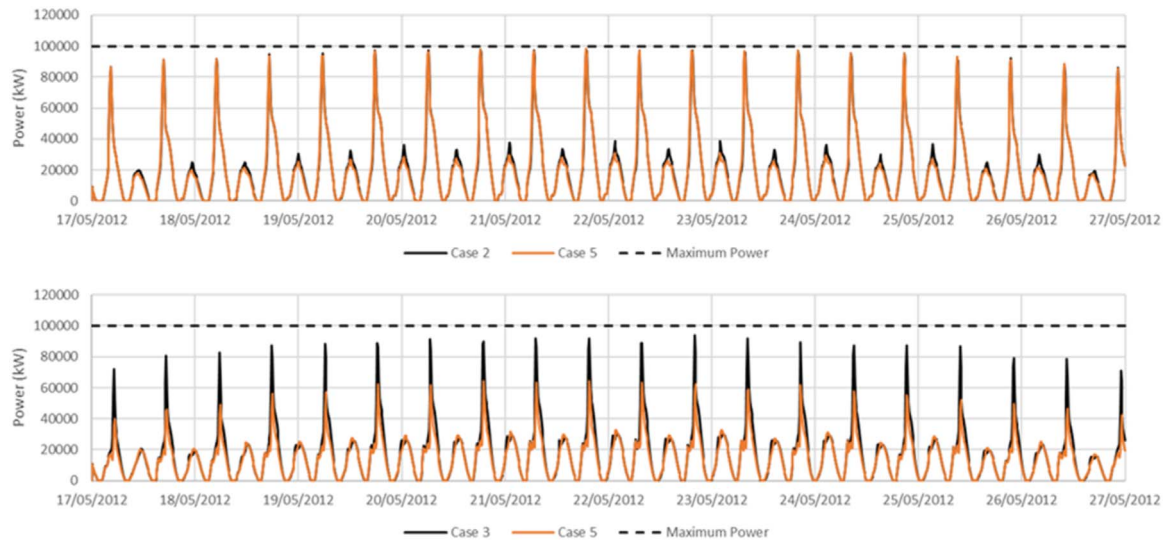
Fig. 10. Total power production for Fair Head (top) and Torr Head (bottom). The solid black line represents the power production from each array separately (case 2 & 3) and the solid orange represents both Fair Head and Torr Head operating concurrently (case 5). The dash black line represents the maximum total power output of each array.

in this area. However, the magnitude of bed shear stress increase is similar in both cases 2 and 8. The maximum increase in bed shear stress for case 8 is 4.5 Pa. For case 2 it is 4.0 Pa. The mean increase in both cases is 0.7 Pa. Whilst the seabed around Fair Head and Torr Head is mainly gravel, 40 km to the west is the Skerries and Causeway Special Area of Conservation (SAC). One of the primary designations of the SAC was the protection of sandbanks. It has been shown that tidal stream devices can influence the maintenance of sandbanks (Neill et al., 2012). In this case study, the effect should be minimal. The net transport of sediment to the SAC is from the west (Pingree and Griffiths, 1979) and the large tidal asymmetry means any accumulation within the vicinity of the tidal array should transport eastwards. However, the only way to be certain is to use the methodology shown in (Robins et al., 2014), which can determine the array size that would not cause an impact above natural variation is sediment transport.

There is a clear interaction between Fair Head and Torr Head. This is due to their proximity and installed capacity. Likewise, with the lack of interaction with the other six sites. The installed capacity of the other sites is significantly smaller than Fair Head and Torr Head. Thus, their zone of influence is much smaller. Although, not investigated, the interaction between Ramsey Sound, Anglesey and Fair/Torr Head, would likely be minimal if their rated capacity were all equal. This is due to distances between the sites. It is approximately 175 km between Ramsey Sound and Anglesey and 225 km between Anglesey and Fair/Torr Head. The risk of

interaction to these sites will be when more intermediary sites are developed. The risk of interaction between other forms of energy extraction in the Irish Sea, i.e. offshore wind and tidal barrages, will be of little risk. The reduction in tidal velocities due to wind turbine monopile structures is negligible (Zhang et al., 2009). There is no interaction between tidal stream devices and tidal barrages in the Irish Sea (Wilson et al., 2012). Whilst the deployment of tidal stream extraction remains small, ~10 MW, the risk of interaction within the Irish Sea is small. As the industry grows and the technology matures, allowing sites with lower peak velocities to be exploited, the risk of interaction will grow. Other tidal sites, such as in the Pentland Firth, where there are four proposed projects geographically within 20 km of each other, the potential for interaction is significantly higher.

9. Conclusions

A cumulative impact assessment of eight tidal stream developments, totaling 264 MW, in the Irish Sea has been undertaken using a high-resolution depth-averaged hydrodynamic model. Results show that five of the eight tidal projects run quite independently of each other. However, projects at Fair Head, Torr Head and Mull of Kintyre lie within each other's zone of influence. Due to the computational expense of running the model, a second smaller model was developed which included only these three projects.

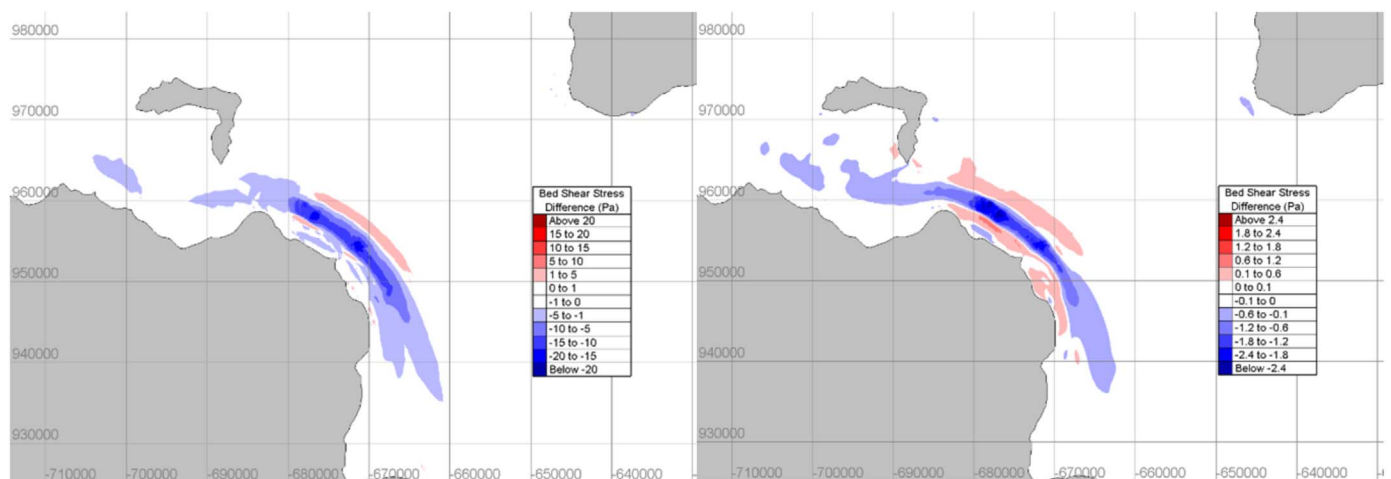Results of the second model show that the Mull of Kintyre project

Fig. 11. Variation in maximum bed shear stress (left) and mean bed shear stress (right) for case 8.
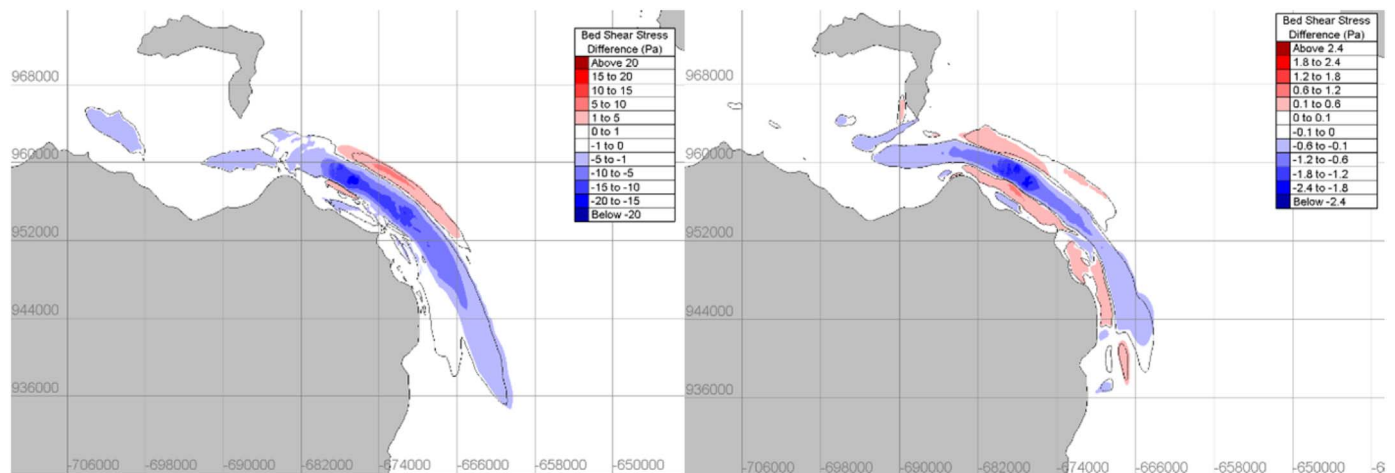
Fig. 12. Variation in maximum bed shear stress (left) and mean bed shear stress (right) for case 2. The black contour represents the spatial extent of change for case 8.

had very little impact on the energy production at Fair Head and Torr Head. Energy production slightly increased (+0.09%) at the Mull of Kintyre with the presence of the other two projects. For the two remaining projects, Fair Head had a greater impact on Torr Head than the other way. Torr Head reduces energy production at Fair Head by 2%, whereas Fair Head reduces energy production by 17% at Torr Head. On closer examination, this is due to the tidal asymmetry at the site. The flood (west-east) is stronger than the ebb. As Fair Head lies to the west of Torr Head, the impact is greater. Despite both arrays having an installed capacity of 100 MW, the maximum power during the flood tide is 98.1 MW for Fair Head and 64.5 MW for Torr Head. Due to the intra-array effects, the total maximum power output is 97.8 MW for Fair Head and 93.8 MW for Torr Head, when operated separately. This represents a 31% reduction in peak power output at Torr Head.

Whilst the economics may allow Fair Head to operate commercially with a slight reduction in energy production, a further detailed analysis would be required to determine if Torr Head remains economically viable. However, if Torr Head can still operate commercially in the presence of Fair Head, then the additional environmental impact of Torr Head, such as the change in bed shear stress, is small.

Within the Irish Sea, very few tidal projects investigated are geographically within close proximity of each other, meaning their interaction is limited. Whilst the deployment of tidal stream extraction remains small, ~10 MW, the risk of interaction within the Irish Sea is small. As the industry grows and the technology matures, allowing sites with lower peak velocities to be exploited, the risk of interaction to these sites will grow when more intermediary sites are developed.

Acknowledgment

References

Ahmadian, R., Falconer, R., Bockelmann-Evans, B., 2012. Far-field modelling of the hydro-environmental impact of tidal stream turbines. Renew. Energy 38 (1), 107–116.
British Oceanographic Data Centre, Tidal observations, [Online], Available: ⟨http://www.bodc.ac.uk/⟩.
Couch, S.J., Bryden, I.G., 2007. Large-scale physical response of the tidal system to energy extraction and its significance for informing environmental and ecological impact assessment. In: Proceedings Oceans 2007-Europe International Conference 2007, pp. 912–916.
Davies, A.M., Jones, J.E., 1992. A three dimensional model of the M2, S2, N2, K1 and O1 tides in the Celtic and Irish Seas. Progress. Oceanogr. 29 (3), 197–234.
Draper, S., Adcock, T.A., Borthwick, A.G., Houlsby, G.T., 2014. Estimate of the tidal stream power resource of the Pentland Firth. Renew. Energy 63, 650–657.
EMEC, 2009. Assessment of Tidal Energy Resource, [Online], Available: ⟨http://www.emec.org.uk/assessment-of-tidal-energy-resource/⟩.
Fairley, I., Masters, I., Karunarathna, H., 2015. The cumulative impact of tidal stream turbine arrays on sediment transport in the Pentland Firth. Renew. Energy 80, 755–769.
Gunn, K., Stock-Williams, C., 2013. On validating numerical hydrodynamic models of complex tidal flow. Int. J. Mar. Energy 3, e82–e97.
Hashemi, M.R., Neill, S.P., Robins, P.E., Davies, A.G., Lewis, M.J., 2015. Effect of waves on the tidal energy resource at a planned tidal stream array. Renew. Energy 75, 626–639.
Jones, J.E., 1983. Charts of the O1, K1, N2, M2 and S2 tides in the Celtic Sea including M2 and S2 tidal currents. Institute of Oceanographic Sciences, (Report No.169).
Lewis, M., Neill, S.P., Robins, P.E., Hashemi, M.R., 2015. Resource assessment for future generations of tidal-stream energy arrays. Energy 83, 403–415.
Martin-Short, R., Hill, J., Kramer, S.C., Avdis, A., Allison, P.A., Piggott, M.D., 2015. Tidal resource extraction in the Pentland Firth, UK: potential impacts on flow regime and sediment transport in the Inner Sound of Stroma. Renew. Energy 76, 596–607.
Neill, S.P., Jordan, J.R., Couch, S.J., 2012. Impact of tidal energy converter (TEC) arrays on the dynamics of headland sand banks. Renew. Energy 37 (1), 387–397.
Neill, S.P., Hashemi, M.R., Lewis, M.J., 2014. Optimal phasing of the European tidal stream resource using the greedy algorithm with penalty function. Energy 73, 997–1006.
Neill, Simon P., Vögler, Arne, Goward-Brown, Alice J., Baston, Susana, Lewis, Matthew J., Gillibrand, Philip A., Waldman, Simon, Woolf, David K., 2017. The wave and tidal resource of Scotland. Renew. Energy. http://dx.doi.org/10.1016/j.renene.2017.03.027, ISSN 0960–1481, (Available online 16 March 2017).
OSU Tidal Data Inversion, [Online], Available: ⟨http://volkov.oce.orst.edu/tides/⟩.
Pingree, R.D., Griffiths, D.K., 1979. Sand transport paths around the British Isles resulting from M 2 and M 4 tidal interactions. J. Mar. Biol. Assoc. U. Kingd. 59 (02), 497–513.
Pingree, R.D., Griffiths, D.K., 1987. Tidal friction for semidiurnal tides. Cont. shelf Res. 7 (10), 1181–1209.
Plew, D.R., Stevens, C.L., 2013. Numerical modelling of the effect of turbines on currents in a tidal channel – Tory Channel, New Zealand. Renew. Energy 57, p269–282.
Rastogi, A.K., Rodi, W., 1978. Predictions of heat and mass transfer in open channels. J. Hydraul. Div. 104 (3), 397–420.
RenewableUK, 2015. Wave and Tidal Energy in the UK – Capitalising on Capability, [Online], Available: ⟨http://www.renewableuk.com/en/publications/index.cfm/⟩.
Robins, P.E., Neill, S.P., Lewis, M.J., 2014. Impact of tidal-stream arrays in relation to the natural variability of sedimentary processes. Renew. Energy 72, 311–321.
Robins, P.E., Neill, S.P., Lewis, M.J., Ward, S.L., 2015. Characterising the spatial and temporal variability of the tidal-stream energy resource over the northwest European shelf seas. Appl. Energy 147, 510–522.
Robinson, I.S., 1979. The tidal dynamics of the Irish and Celtic Seas. Geophys. J. Int. 56 (1), 159–197.
Telemac, [Online], Available: ⟨http://www.opentelemac.org/⟩.
Tidal Ventures, 2015. Torr Head Tidal Energy Array EIA, [Online], Available: ⟨http://www.tidalventures.com/downloads/environmentalstatement/ES_9_Benthic & IntertidalEcology.pdf⟩.
Walkington, I., Burrows, R., 2009. Modelling tidal stream power potential. Appl. Ocean Res. 31 (4), 239–245.
Wilson, S., Bourban, S., Couch, S., 2012. Understanding the interactions of tidal power projects across the UK continental shelf. In: Proceedings of the 4th International Conference on Ocean Energy, Dublin.
Woolf, D.K., 2013. The strength and phase of the tidal stream. Int. J. Mar. Energy 3, 4.
Young, E.F., Aldridge, J.N., Brown, J., 2000. Development and validation of a three-dimensional curvilinear model for the study of fluxes through the North Channel of the Irish Sea. Cont. Shelf Res. 20 (9), 997–1035.
Zhang, W., Xia, H., Wang, B., 2009. Numerical Calculation of the Impact of Offshore Wind Power Stations on Hydrodynamic ConditionsAdvances in Water Resources and Hydraulic Engineering. Springer, Berlin, Heidelberg.